REGULAR ARTICLE

Design and synthesis of a stereodynamic catalyst with reversal of selectivity by enantioselective self-inhibition

Jan Felix Scholtes[1,2] | Oliver Trapp[1,2] (ID)

[1] Department of Chemistry, Ludwig-Maximilians-University Munich, Munich, Germany

[2] Max-Planck-Institute for Astronomy, Heidelberg, Germany

Correspondence
Prof. Dr Oliver Trapp, Department of Chemistry, Ludwig-Maximilians-University Munich, Butenandtstr. 5-13, 81377 Munich, Germany.
Email: oliver.trapp@cup.uni-muenchen.de

Funding information
H2020 European Research Council, Grant/Award Number: AMPCAT 258740; Max-Planck-Gesellschaft, Grant/Award Number: Max-Planck-Fellow; Max-Planck-Society; European Research Council (ERC), Grant/Award Number: 258740

Abstract

Chirality plays a pivotal role in an uncountable number of biological processes, and nature has developed intriguing mechanisms to maintain this state of enantiopurity. The strive for a deeper understanding of the different elements that constitute such self-sustaining systems on a molecular level has sparked great interest in the studies of autoinductive and amplifying enantioselective reactions. The design of these reactions remains highly challenging; however, the development of generally applicable principles promises to have a considerable impact on research of catalyst design and other adjacent fields in the future. Here, we report the realization of an autoinductive, enantioselective self-inhibiting hydrogenation reaction. Development of a stereodynamic catalyst with chiral sensing abilities allowed for a chiral reaction product to interact with the catalyst and change its selectivity in order to suppress its formation, which caused a reversal of selectivity over time.

KEYWORDS
asymmetric catalysis, autoinduction, chirality transfer, ligand design, noncovalent interaction, tropos ligands

1 | INTRODUCTION

The basis of an autoinductive, asymmetric reaction is the participation of the chiral product in its own formation. This may involve the incorporation of the product into a larger catalyst structure or catalytic activity of the product molecules themselves.[1] A self-amplifying reaction also necessitates occurrence of nonlinear effects,[2] which can lead to a significant growth of the enantiomeric excess as demonstrated first by Kagan and Noyori.[3-5] Along similar lines, Mikami and coworkers applied concepts of stereoselective activation and deactivation by combining racemic ligands with chiral coligands to induce enantioselectivity in various transformations.[6-8]

Even before the first experimental realization of stereoamplification, Frank described a "mutual antagonism," where the desired reaction is assisted by the inducing product and the undesired reaction is simultaneously suppressed in order to prevent a decrease in selectivity, as a fundamental requirement.[9]

The first experimental examples that combine autoinduction and amplification were delivered by Wynberg and Alberts and later by Wynberg and Feringa, who observed autoinductive properties during C—C bond formation.[10,11] Danda et al[12] and Shvo et al[13] performed enantioselective hydrocyanation reactions on aldehydes incorporating the reaction products into the chiral catalysts, while Figadère et al[14] reported autoinductive aldol

reactions between 2-trimethylsilyloxyfuran and various aldehydes in the presence of a BINOL-Ti catalyst. The most prominent example is the Soai reaction, a self-amplifying, autocatalytic reaction in which substituted 5-pyrimidinecarbaldehydes react with diisopropylzinc to form the corresponding pyrimidyl alcohols. Catalyzed by zinc complexes of the same alcohol, even very small enantiomeric surpluses in the latter are sufficient to alkylate aldehydes with high enantioselectivities.[15,16]

Recently, we developed a self-amplifying, asymmetric hydrogenation reaction for prochiral olefins.[17] It features a *tropos* biphenyl-based ligand[18-22] with a low barrier of inversion.[17,23] The ligand backbone was modified with interaction sites for efficient noncovalent bonding,[24,25] which were derived from a chiral recognition system developed by Pirkle and Murray.[26-28] During the course of the reaction, enantioselective, noncovalent interactions between chiral reaction products and the interaction sites on the rhodium catalyst induce changes in the complex structure, thus enhancing the catalyst's selectivity in subsequent turnovers.[17] The most crucial requirements for this system include (a) constant adaptation to changing equilibria which is provided by the dynamic nature of noncovalent interactions between catalyst and reaction product, (b) the rapid incorporation of the chiral reaction product into the reaction cycle of a comparatively slower hydrogenation reaction, (c) the enantioselectivity of the interaction between selector and product molecules, which created the basis for mutual antagonism, and (d) a fast stereochemical response during product-selector interaction that leads to immediate structural change in the catalyst.

We believed that a reaction featuring an autoinductive, self-inhibiting process based on the same prerequisites would be of equal interest due to its complementary, "inverse" nature (see Figure 1). Earlier studies have shown that stereodynamic 3,3′-methoxy-2,2′-biphenol-based ligands with (S)-amino acid-derived interaction sites (selectors) in the 5,5′-position can be aligned by other (S)-amino acid-derived diamides to induce the opposite stereo information during subsequent asymmetric hydrogenation reactions. Diamide selectors were found to interact in a highly enantioselective manner; however, overly efficient binding resulted in the formation of supramolecular ligand adducts and a concurrent loss of ligand's stereo dynamics.[29,30] As a consequence, ligands with the same biphenyl core, decorated with (S)-phenylalanine-derived amido ester groups, were to be investigated. These were believed to be able to differentiate the chirality of structurally similar molecules in their surroundings.[31] Enantioselective interaction with amino acid derivatives of the same configuration was envisioned to induce a change of the ligand's rotameric ratio, while not adversely affecting the fluxional nature of the stereodynamic ligand core. In a two-stage development process, it was decided to (a) conduct interaction studies with ligands and different chiral additives to evaluate the degree of chirality transfer[32,33] and subsequently (b) apply these results to design an autoinductive, self-inhibiting, rhodium-catalyzed hydrogenation reaction, where reduction of an appropriately substituted olefin would yield amino acid-derived reaction products capable of changing the catalysts selectivity.[34]

2 | MATERIALS AND METHODS

2.1 | General methods

All reactions involving the use of oxygen and/or moisture sensitive substances were carried out in heat dried glassware under an atmosphere of nitrogen or argon using
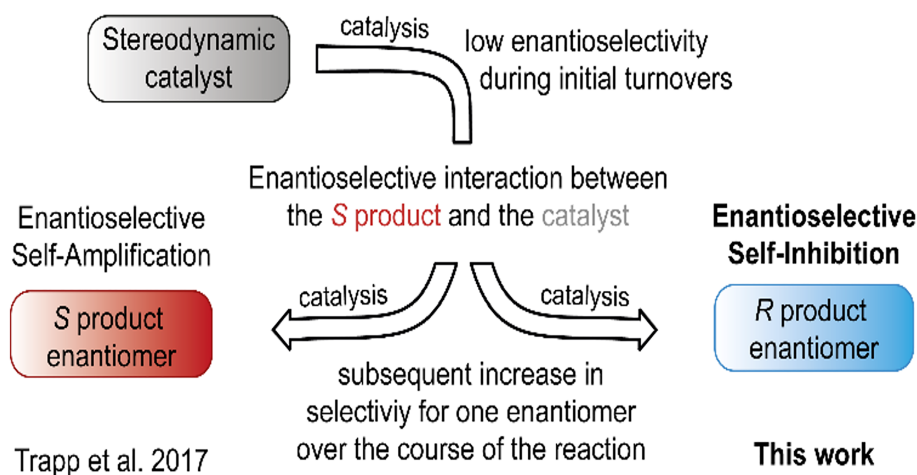

FIGURE 1 Conceptual representation of two types of autoinductive catalytic reactions that have been studied in the Trapp group and that feature either enantioselective self-amplification or enantioselective self-inhibition

standard Schlenk techniques. All chemicals were used as received from suppliers without further purification. Column chromatography was done using silica gel (technical grade, pore size 60 Å, 70-230 mesh, 63-200 μm) produced by Sigma-Aldrich Chemie GmbH. Thin layer chromatography was performed on coated aluminum sheets (Machery-Nagel POLYGRAM SIL G/UV 254). Components were visualized by fluorescence quenching during irradiation with UV light (254 nm). Dry solvents were taped from solvent purification system MB SPS-800 and used immediately. Dry and stabilized THF (250 ppm butylated hydroxytoluene) was purchased from Sigma-Aldrich Chemie GmbH. Manual degassing of solvents, if needed, was done by performing three consecutive freeze-pump-thaw cycles. Oxygen-free solvents were then placed under an atmosphere of argon.

NMR spectra were recorded on Varian NMR-System (300, 400, and 600 MHz) and Bruker Avance III HD and DRX (300, 400, 600, and 800 MHz). NMR shifts are given in parts per million (ppm) and are referenced to the residual proton or carbon solvent signals.[35] Multiplicity is termed as follows: s (singlet), bs (broad singlet), d (doublet), t (triplet), q (quartet), quint (quintet), sept (septet), dd (doublet of a doublet), dt (doublet of triplet) and tt (triplet of triplet), and m (multiplet). Assignment was done by means of two-dimensional experiments (^{1}H-^{1}H-COSY, ^{1}H-^{13}C-HSQC, and ^{1}H-^{13}C-HMBC). Mass spectra were acquired on Thermo Finnigan LTQ FT Ultra FT-ICR (ESI) or Thermo Q Finnigan MAT 95 (EI). For solid-state IR analysis, Thermo Fisher Nicolet 6700 FT-IR-Spectrometer was employed, and the wavenumber of reflectance was measured with signals being denoted as s (strong), m (medium), w (weak), and b (broad). Elemental analysis was conducted on an Elementar vario micro cube equipped with a thermal conductivity detector.

2.2 | Dimethyl 6,6′-bis (allyloxy)-5,5′-dimethoxy-[1,1′-biphenyl]-3,3′-dicarboxylate (2)

This compound was prepared according to a known procedure.[36] Unprotected biphenol was prepared from methyl vanillate according to literature.[37] The biphenol (8.00 g, 22.1 mmol, 1.00 eq.) and potassium carbonate (30.5 g, 221 mmol, 10.0 eq.) were suspended in 2-butanone (250 mL). Allyl bromide (9.55 mL, 110 mmol, 5.00 eq.) was added, and the mixture was refluxed for 24 hours. All volatiles were subsequently evaporated, and the solid residue was heated to 70°C for 1 hour under vacuum to remove residual allyl bromide. Solids were then partitioned between ethyl acetate (200 mL) and water (200 mL), layers were separated, and the aqueous layer

was re-extracted with more ethyl acetate (twice with 100 mL each). Combined organic layers were washed with brine (100 mL), dried over sodium sulfate, and evaporated to give a yellow oil, which crystallized into an off-white solid upon prolonged drying in high vacuum (9.46 g, 22.1 mmol, 97%). ^{1}H NMR (CDCl$_3$, 598.76 MHz, 300 K): δ = 3.88 (s, 3H), 3.93 (s, 6H), 4.43-4.45 (m, 2H), 4.99-5.02 (m, 1H), 5.05-5.09 (m, 1H), 5.71-5.79 (m, 1H), 7.60 (d, 1H, ^{4}J(H,H) = 2.0 Hz), 7.61 (d, 1H, ^{4}J(H,H) = 2.0 Hz) ppm. ^{13}C{^{1}H} NMR (CDCl$_3$, 150.57 MHz, 300 K): δ = 52.2, 56.2, 74.1, 113.0, 117.5, 125.2, 125.3, 132.3, 134.0, 150.1, 152., 166.8 ppm. HRMS (ESI): m/z calcd. for C$_{24}$H$_{30}$N$_1$O$_8$ [M + NH$_4$]$^+$: 460.1966; found: 460.1971. FTIR: ṽ = 761 (s), 981 (s), 1042 (s), 1173 (s), 1222 (s), 1286 (s), 1714 (s), 2845 (w), 2870 (w), 2951 (m), 3015 (w), 3090 (w) cm^{-1}.

2.3 | 6,6′-Bis (allyloxy)-5,5′-dimethoxy-[1,1′-biphenyl]-3,3′-dicarboxylic acid (3)

Diester 2 (9.40 g, 21.2 mmol, 1.00 eq.) and sodium hydroxide (8.50 g, 212 mmol, 10.0 eq.) were dissolved in a mixture of water (110 mL) and THF (110 mL), and the biphasic system was refluxed under vigorous stirring for 14 hours. For work-up, THF was evaporated, and the aqueous orange solution was acidified with conc. HCl solution (6 M) until pH 1 was reached and a thick, white precipitate formed. The solids were filtered off and washed with more water to neutrality. Freeze-drying afforded product as a white powder (8.80 g, 21.2 mmol, 99%). ^{1}H NMR (CDCl$_3$, 800.34 MHz, 300 K): δ = 3.90 (s, 3H), 4.37 to 4.38 (m, 2H), 4.99 to 5.01 (m, 1H), 5.04 to 5.06 (m, 1H), 5.68 to 5.73 (m, 1H), 7.41 (d, 1H, ^{4}J(H,H) = 2.0 Hz), 7.57 (d, 1H, ^{4}J(H,H) = 2.0 Hz), 12.91 (bs, 1H) ppm. ^{13}C{^{1}H} NMR (CDCl$_3$, 201.24 MHz, 300 K): δ = 55.9, 73.2, 112.8, 117.1, 124.3, 125.7, 131.5, 134.1, 149.0, 152.1, 166.8 ppm. HRMS (ESI): m/z calcd. for C$_{22}$H$_{26}$NO$_8$ [M + NH$_4$]$^+$: 432.16529; found: 432.16564. FTIR: ṽ = 759 (s), 980 (s), 1040 (s), 1179 (s), 1218 (s), 1285 (s), 1404 (s), 1577 (s), 1677 (s), 2519 (bm), 2837 (bm), 2970 (bm), 3063 (w) cm^{-1}.

2.4 | Di-*tert*-butyl 2,2′-((6,6′-bis (allyloxy)-5,5′-dimethoxy-[1,1′-bi-phenyl]-3,3′-dicarbonyl)bis (azanediyl))(2S,2′S)-bis(3-phenylpropanoate) (4a)

Dicarboxylic acid 3 (4.00 g, 9.65 mmol, 1.00 eq.) was placed in a dried Schlenk flask with reflux condenser and overpressure ventilation, and thionyl chloride (30 mL) was added. The mixture was refluxed for 7 hours and turned unto a clear, brown solution within minutes.

Subsequently, thionyl chloride was removed in vacuo, residual solids were suspended in dry toluene (15 mL), and all volatiles were removed again. The last two steps were repeated another two times, and after drying, the product was obtained as a grey solid. Allyl-protected acid chloride (800 mg, 4.43 mmol, 2.50 eq.) was dissolved in dry DCM (4 mL). In a separate flask, phenylalanine *tert*-butyl ester hydrochloride (1.14 g, 4.43 mmol, 2.50 eq.) was mixed with diisopropylethylamine (1.54 mL, 8.86 mmol, 5.00 eq.) in dry DCM (10 mL) to give a clear solution. Both mixtures were cooled in an ice bath, and the acid chloride was subsequently added dropwise to the selector solution. The resulting orange solution was slowly warmed to room temperature, and stirring was continued for 18 hours. For work-up, the mixture was diluted with ethyl acetate (120 mL) and subsequently washed with HCl solution (2 M, 3 120 mL), saturated bicarbonate solution (2 × 120 mL), and brine (120 mL), dried over sodium sulfate and evaporated to yield the product as a brown powder (1.33 g, 1.62 mmol, 91%). ^{1}H NMR (CDCl$_3$, 598.47 MHz, 300 K): δ = 1.39 (s, 9H), 3.14 to 3.26 (m, 2H), 3.89 (s, 3H), 4.35 to 4.36 (m, 2H), 4.96 to 5.05 (m, 2H), 5.05 (s, 1H), 5.70 to 5.77 (m, 1H), 7.16 to 7.28 (m, 6H), 7.43 (s, 1H) ppm. The NH protons were not observed. ^{13}C{^{1}H} NMR (CDCl$_3$, 150.57 MHz, 300 K): δ = 28.1, 28.3, 54.5, 56.1, 74.1, 82.3, 111.7, 117.5, 121.2, 127.0, 128.3, 128.8, 129.5, 132.1, 134.0, 136.7, 148.7, 152.9, 166.2, 171.6 ppm. HRMS (ESI): m/z calcd. for C$_{48}$H$_{57}$N$_2$O$_{10}$ [M + H]$^+$: 821.4008; found: 821.4026. FTIR: ṽ = 698 (s), 982 (s), 1151 (s), 1219 (s), 1366 (s), 1537 (s), 1639 (s), 1706 (s), 2867 (w), 2935 (w), 2978 (w), 3029 (w), 3062 (w), 3344 (bm) cm^{-1}.

2.5 | Di-*tert*-butyl 2,2′-((6,6′-dihydroxy-5,5′-dimethoxy-[1,1′-biphenyl]-3,3′-dicarbonyl) bis (azanediyl))(2S,2′S)-bis(3-phenylpropanoate) (5a)

The deprotection was done by a known procedure, which was slightly modified.[38] To remove the allyl groups, substrate **4a** (750 mg, 914 mmol, 1.00 eq.), palladium acetate (10.2 mg, 45.7 µmol, 0.05 eq.), and (4-dimethylaminophenyl)-diphenylphosphine (140 mg, 457 µmol, 0.50 eq.) were dissolved in dry ethyl acetate (18 mL), and the suspension was stirred for 15 minutes. The resulting solution was treated with formic acid (0.20 mL, 5.30 mmol, 5.80 eq.), and the orange mixture was subsequently refluxed. It quickly turned brown and gas evolved. After 2 hours, the mixture was cooled to room temperature and diluted with ethyl acetate (80 mL). The organic layer was washed with HCl solution (2 M, 4 × 100 mL), saturated bicarbonate solution (3 × 100 mL)

and brine (1 × 100 mL), dried over sodium sulfate, and evaporated on celite. Purification by column chromatography (silica, *n*-pentane:ethyl acetate 1:2, R$_f$ = 0.4). Appropriate fractions were evaporated, and the residue precipitated from ethyl acetate:n-pentane to yield the desired diol **5a** as an off-white powder (481 mg, 649 µmol, 71%). ^{1}H NMR (CDCl3, 598.74 MHz, 300 K): δ = 1.39 (s, 9H), 3.13-3.23 (m, 2H), 3.90 (s, 3H), 5.03-5.04 (m, 1H), 6.20 (bs, 1H), 7.17-7.23 (m, 5H), 7.27 (s, 1H), 7.30 (s, 1H), 7.39 (s, 1H) ppm. ^{13}C{^{1}H} NMR (CDCl$_3$, 150.57 MHz, 300 K): δ = 55.9, 73.2, 112.8, 117.1, 124.3, 125.7, 131.5, 134.1, 149.0, 152.1, 166.8 ppm. HRMS (ESI): m/z calcd. for C$_{42}$H$_{49}$N$_2$O$_{10}$ [M + H]$^+$: 741.3382; found: 741.3391. FTIR: ṽ = 698 (s), 1042 (s), 1086 (s), 1150 (s), 1220 (s), 1366 (s), 1487 (s), 1593 (s), 1636 (s), 1710 (s), 2933 (m), 2977 (m), 3029 (w), 3330 (bm), 3508 (bw) cm^{-1}.

2.6 | Di-*tert*-butyl 2,2′-((6,6′-bis ((diphenylphosphaneyl)oxy)-5,5′-dimethoxy-[1,1′-biphenyl]-3,3′-dicarbonyl) bis (azanediyl))-(2S,2′S)-bis(3-phenylpropanoate) (6a)

Selector-modified diol **5a** (350 mg, 472 µmol, 1.00 eq.) and 1,4-diazabicyclo[2.2.2]octane (DABCO, 212 mg, 1.89 mmol, 4.00 eq.) were placed in a flame-dried Schlenk flask and dissolved in dry and degassed DCM (10 mL). The solution was cooled in an ice bath and PPh$_2$Cl (326 µL, 1.89 mmol, 4.00 eq.) was added. After 15 minutes, the ice bath was removed, and stirring was continued at room temperature for another 2 hours. For work-up, all volatiles were removed, and the off-white residue was suspended in dry, degassed, and stabilized THF (5 mL). The suspension was filtered through an inert pad of neutral alumina, and the product was eluted with more THF. Combined fractions were evaporated to give a white foam. Re-precipitation from DCM:n-pentane (4x, 1:10 mL) gave the desired phosphinite **6a** as a white powder (105 mg, 94.8 mmol, 20%). The compounds exist as two interconverting rotamers. The minor isomer (A, S_{ax}) shows sharp NMR signals in ^{31}P, ^{1}H, and ^{13}C NMR spectra. For the major rotamer (B, R_{ax}), significant line broadening was detected in ^{31}P and ^{1}H NMR spectra, and even with concentrated samples, almost no peaks could be detected in the ^{13}C NMR spectrum. ^{1}H NMR (THF-d_8, 400.22 MHz, 300 K): δ = 1.37 (s, B), 1.39 (s, A), 3.04-3.09 (m, A), 3.12 (bs, B), 3.14-3.19 (m, A), 3.27 (bs, B), 3.53 (bs, B), 3.59 (s, A), 4.75-4.81 (m, A) 4.86 (bs, B), 6.91 (bs, B), 7.04-7.26 (m, A and B), 7.12 (m, A), 7.28-7.35 (m, A), 7.35 (d, ^{4}J(H,H) = 1.9 Hz, A), 7.40 (d, ^{3}J(H, H) = 7.7 Hz, A), 7.48 (bs, B), 8.47 (bs, B) ppm. ^{13}C{^{1}H} NMR (THF-d_8, 100.54 MHz, 300 K): δ = 27.2, 37.5, 54.4,

54.7, 54.9, 80.5, 111.8, 121.1, 120.8, 126.3, 126.2, 127.3, 127.3, 127.4, 127.5, 127.5, 127.5, 127.9, 129.1, 129.2, 129.3, 129.5, 129.5, 129.7, 130.3, 130.5, 130.6, 130.7, 131.3, 137.7, 138.0, 142.5, 142.7, 143.0, 143.1, 147.5, 151.2, 165.0, 165.1, 170.8 ppm. $^{31}P\{^1H\}$ NMR (THF-d_8, 161.85 MHz, 300 K): δ = 118.4 (bs, 1P, B), 121.1 (s, 1P, A), 121.1 (bs, 1P, B) ppm. HRMS (ESI): m/z calcd. for $C_{66}H_{67}N_2O_{10}P_2$ [M + H]$^+$: 1109.4271; found: 1109.4286. FTIR: $\tilde{v}$ = 694 (s), 863 (m), 1094 (s), 1152 (s), 1367 (s), 1476 (s), 1642 (s), 1707 (s), 2859 (w), 1933 (w), 2977 (w), 3054 (w), 3349 (bm) cm^{-1}.

2.7 | [Rh(6a)(COD)]BF$_4$ (7a)

Bisphosphinite **6a** (53 mg, 47.8 μmol, 1.00 eq.) and [Rh (COD)$_2$]BF$_4$ (19.4 mg, 47.8 μmol, 1.00 eq.) were placed in a flame-dried Schlenk flask and dissolved in dry and degassed DCM (3.5 mL). The clear orange solution was stirred for 2 hours at room temperature and then concentrated to 1.0 mL. Addition of dry and degassed pentane (10 mL) gave an orange precipitate. The supernatant solution was removed using a filter-tipped cannula, and re-precipitation was repeated another two times. The solids were finally dried in high vacuum to give the desired Rh complex as a yellow powder (61.0 mg, 43.4 μmol, 91%). The compound exists as two interconverting rotamers. $^{31}P\{^1H\}$ NMR (CDCl$_3$, 161.98 MHz, 300 K): δ = 127.91 (d, ^1J(P,Rh) = 179.9 Hz, S$_{ax}$), 128.02 (d, ^1J(P,Rh) = 181.3 Hz, R$_{ax}$) ppm. EA (CHNS): calcd. for $C_{74}H_{78}N_2O_{10}P_2$RhBF$_4$: C: 63.17, H: 5.59, N: 1.99; found: C: 61.24, H: 5.48, N: 1.93. HRMS (ESI): m/z calcd. for $C_{74}H_{78}N_2O_{10}P_2$Rh [M-BF$_4^-$]$^+$: 1319.4181; found: 1319.4175. FTIR: $\tilde{v}$ = 695 (s), 745 (s), 1039 (s), 1095 (s), 1154 (s), 1215 (m), 1368 (m), 1464 (m), 1585 (m), 1731 (m), 2932 (w), 1376 (w), 3031 (w), 3358 (bm) cm^{-1}.

2.8 | (S)-N-(tert-butyl)-2-hydroxy-3-phenylpropanamide (S1)

(S)-3-Phenyl lactic acid (5.00 g, 30.1 mmol, 1.00 eq.) and hydroxybenzotriazole (4.47 g, 33.1 mmol, 1.10 eq.) were dissolved in dry DMF (60 mL). Diisopropylethyl amine (10.5 mL, 60.2 mmol, 2.00 eq.) was added, the solution was cooled in an ice bath, and 3-(Ethyliminomethyleneamino)-N,N-dimethylpropan-1-amine hydro chloride (EDCI.HCl, 6.34 g, 33.1 mmol, 1.10 eq.) was added. After 15 minutes, all solids had dissolved, and the solution was treated with tert-butyl amine (3.48 mL, 33.1 mmol, 1.10 eq.). After 30 minutes at lower temperatures, the mixture was warmed to room temperature again, and stirring was continued for 18 hours. The mixture was subsequently diluted with ethyl acetate (500 mL) and

washed with HCl solution (2 M, 3 × 300 mL), saturated bicarbonate solution (3 × 300 mL), and brine (1 × 300 mL), dried over sodium sulfate and evaporated to give the product as a yellow oil, which crystallized into an amorphous solid after prolonged drying (4.57 g, 20.7 mmol, 69%). ^1H NMR (CDCl$_3$, 800.34 MHz, 300 K): δ = 1.29 (s, 9H), 2.78 (bs, 1H), 2.93 (dd, 1H, ^2J(H,H) = 13.9 Hz, ^3J(H,H) = 7.6 Hz), 3.12 (dd, 1H, ^2J(H,H) = 13.9 Hz, ^3J(H,H) = 4.8 Hz), 4.16 (dd, 1H, ^3J(H,H) = 7.6 Hz, ^3J(H, H) = 4.9 Hz), 6.13 (s, 1H), 7.24 to 7.26 (m, 3H), 7.30 to 7.32 (m, 2H) ppm. $^{13}C\{^1H\}$ NMR (CDCl$_3$, 201.24 MHz, 300 K): δ = 28.7, 41.1, 51.1, 72.9, 127.1, 128.8, 129.8, 137.1, 172.0 ppm. HRMS (ESI): m/z calcd. for $C_{13}H_{18}NO_2$ [M + H]$^+$: 220.1343; found: 220.1344. FTIR: $\tilde{v}$ = 697 (s), 742 (s), 1089 (s), 1186 (s), 1223 (s), 1454 (s), 1528 (s), 1642 (s), 1743 (s), 2929 (m), 2968 (m), 3030 (w), 3063 (w), 3088 (w), 3225 (bs), 3335 (w), 3397 (w) cm^{-1}. $[\alpha]_D^{20}$−56.5 (c 1%, CHCl$_3$).

2.9 | Bis((S)-1-(tert-butylamino)-1-oxo-3-phenylpropan-2-yl) 6,6′-bis (allyloxy)-5,5′-dimethoxy-[1,1′-biphenyl]-3,3′-dicarboxylate (4b)

Dicarboxylic acid 3 (1.00 g, 2.41 mmol, 1.00 eq.), amido alcohol S1 (2.14 g, 9.56 mmol, 4.00 eq.), and N,N-dimethylaminopyridine (59.0 mg, 482 μmol, 0.20 eq.) were mixed in dry DCM (40 mL) and cooled in an ice bath. EDCI.HCl (1.16 g, 6.03 mmol, 2.50 eq.) was added, and the yellow solution was left stirring to warm to room temperature overnight. After 18 hours, the mixture was diluted with ethyl acetate (200 mL) and subsequently washed with HCl solution (2 M, 3 × 180 mL), saturated bicarbonate solution (2 × 180 mL), and brine (180 mL), dried over sodium sulfate, and evaporated. Purification by column chromatography (neutral alumina, diethyl ether:toluene 3:1, R_f = 0.6) yielded the product as a white solid (1.00 g, 1.22 mmol, 50%). ^1H NMR (CDCl$_3$, 598.74 MHz, 300 K): δ = 1.24 (s, 9H), 3.26 to 3.28 (m, 2H), 3.92 (s, 3H), 4.42 to 4.43 (m, 2H), 4.99 to 5.08 (m, 2H), 5.43 to 5.45 (m, 1H), 5.58 (s, 1H), 5.71 to 5.77 (m, 1H), 7.19 to 7.22 (m, 1H), 7.22 to 7.29 (m, 4H), 7.53 (d, 1H ^4J(H,H) = 2.0 Hz), 7.55 (d, 1H, ^4J(H,H) = 2.0 Hz) ppm. $^{13}C\{^1H\}$ NMR (CDCl$_3$, 150.57 MHz, 300 K): δ = 28.7, 38.0, 51.3, 56.2, 74.2, 75.3, 113.2, 117.7, 124.3, 125.4, 127.1, 128.5, 130.0, 132.3, 133.9, 136.2, 150.6, 152.7, 164.9, 168.0 ppm. HRMS (ESI): m/z calcd. for $C_{48}H_{60}N_3O_{10}$ [M + NH$_4$]$^+$: 838.4273; found: 838.4279. FTIR: $\tilde{v}$ = 696 (s), 979 (s), 1169 (s), 1217 (s), 1657 (s), 1711 (s), 2867 (w), 2966 (w), 3029 (w), 3088 (w), 3291 (bm) cm^{-1}.

2.10 | Bis((S)-1-(tert-butylamino)-1-oxo-3-phenylpropan-2-yl) 6,6′-dihydroxy-5,5′-dimethoxy-[1,1′-biphenyl]-3,3′-dicarboxylate (5b)

The deprotection was done by a known procedure, which was slightly modified.[38] To remove the allyl groups, substrate **4b** (890 mg, 1.08 mmol, 1.00 eq.), palladium acetate (12.2 mg, 54.2 µmol, 0.05 eq.), and (4-dimethylaminophenyl)-diphenylphosphine (166 mg, 542 µmol, 0.50 eq.) were dissolved in dry ethyl acetate (18 mL), and the suspension was stirred for 15 minutes. The resulting solution was treated with formic acid (0.24 mL, 6.29 mmol, 5.80 eq.), and the orange mixture was subsequently refluxed. It quickly lost its color and gas evolved. After 1 hour, the mixture was cooled to room temperature and diluted with ethyl acetate (100 mL). The organic layer was washed with HCl solution (2 M, 4 × 100 mL), saturated bicarbonate solution (2 × 100 mL), and brine (1 × 100 mL), dried over sodium sulfate and evaporated. The residue was precipitated from ethyl acetate:n-pentane to yield the desired diol **5b** as an off-white powder (745 mg, 1.01 mmol, 93%). ^{1}H NMR (CDCl$_3$, 598.47 MHz, 300 K): δ = 1.25 (s, 9H), 3.27 (d, 2H, ^{3}J(H,H) = 5.9 Hz), 3.98 (s, 3H), 5.46 (t, 1H, ^{3}J(H,H) = 5.9 Hz), 5.63 (s, 1H), 6.39 (s, 1H), 7.19 to 7.21 (m, 1H), 7.23 to 7.26 (m, 4H), 7.49 (d, 1H, ^{4}J(H,H) = 1.9 Hz), 7.71 (d, 1H, ^{4}J(H,H) = 1.9 Hz) ppm. ^{13}C{^{1}H} NMR (CDCl$_3$, 150.57 MHz, 300 K): δ = 28.7, 38.00, 51.4, 56.5, 75.0, 111.2, 121.0, 122.8, 126.4, 127.0, 128.4, 130.0, 136.3, 146.8, 148.0, 164.9, 168.2 ppm. HRMS (ESI): m/z calcd. for C$_{42}$H$_{52}$N$_3$O$_{10}$ [M + NH$_4$]$^+$: 758.3647; found: 758.3650. FTIR: ṽ = 699 (s), 740 (m), 1039 (m), 1208 (s), 1277 (s), 1454 (m), 1669 (s), 2868 (w), 2933 (w), 2965 (m), 3027 (w), 3065 (w), 3317 (bm), 3407 (w) cm^{-1}.

2.11 | Bis((S)-1-(tert-butylamino)-1-oxo-3-phenylpropan-2-yl) 6,6′-bis((diphenylphosphaneyl)oxy)-5,5′-dimethoxy-[1,1′-biphenyl]-3,3′-dicarboxylate (6b)

Selector-modified diol 5b (50 mg, 67.5 µmol, 1.00 eq.) was dissolved in dry, degassed, and stabilized THF (2 mL), and triethylamine (23.5 µL, 168 µmol, 2.50 eq.) was added. The mixture was cooled in an ice bath, and chlorodiphenylphosphine (24.2 µL, 142 µmol, 2.10 eq.) was added. After 2 hours, the mixture was filtered through a filter-tipped cannula and residual solids rinsed with more THF (2 × 2 mL). Combined organic washings were evaporated, and the resulting white crude product was washed with n-pentane (5 × 2 mL) to give the

product 6b as a white solid (52.0 mg, 46.9 µmol, 69%). Traces of Ph$_2$P(O)PPh$_2$ (side product) still remained and could not be removed without significant loss of product. For some atoms, an additional signal splitting was observed. Those signals are marked X and X′. ^{1}H NMR (THF-d$_8$, 399.78 MHz, 300 K): δ = 1.25 (s, 9H), 3.17 (dd, 2H, ^{2}J(H,H) = 14.8 Hz, ^{3}J(H,H) =, 6.6 Hz), 3.63 (s, 3H), 5.20 (q, ^{3}J(H,H) = 6.3 Hz), 6.53 (s, 1H), 7.03 to 7.32 (m, 15H), 7.30 (s, 1H), 7.38 (d, 1H, ^{4}J(H,H) = 2.0 Hz) ppm. ^{13}C{^{1}H} NMR (THF-d$_8$, 100.54 MHz, 300 K): δ = 27.8, 37.8, 50.3, 54.9, 75.1, 75.2, 112.9, 124.4, 124.7 (J(C,P) = 4.6 Hz), 126.3 (J(C,P) = 11.4 Hz), 127.4 (J(C,P) = 7.4 Hz), 127.6 (J(C,P) = 8.3 Hz), 127.9 (J(C,P) = 4.6 Hz), 128.3 (J(C,P) = 7.4 Hz), 128.8 (J(C,P) = 5.5 Hz), 129.4, 129.5 (J(C,P) = 5.8 Hz), 129.7 (J(C,P) = 11.5 Hz), 130.3 (J(C,P) = 12.9 Hz), 130.5 (J(C,P) = 12.9 Hz), 131.3, 137.0 (J(C,P) = 11.4 Hz), 142.5 (J(C,P) = 17.8 Hz), 142.7 (J(C, P) = 16.6 Hz), 149.0 (J(C,P) = 7.3 Hz), 151.1 ((J(C,P) = 7.4 Hz), 164.2, 167.5, 167.6 ppm. ^{31}P{^{1}H} NMR (THF-d$_8$, 161.85 MHz, 300 K): δ = 122.4 (s), 122.5 (s) ppm. HRMS (ESI): m/z calcd. for C$_{66}$H$_{67}$N$_2$O$_{10}$P$_2$ [M + H]$^+$: 1109.4266; found: 1109.4248. FTIR: ṽ = 692 (s), 1166 (s), 1211 (m), 1453 (m), 1657 (s), 1723 (m), 2867 (w), 2930 (m), 2965 (m), 3002 (w), 3056 (w), 3291 (bm) cm^{-1}.

2.12 | [Rh(6b)(COD)]BF$_4$ (7b)

Bisphosphinite **6b** (33 mg, 29.8 µmol, 1.00 eq.) and [Rh(COD)$_2$]BF$_4$ (9.10 mg, 22.3 µmol, 1.00 eq.) were placed in a dried Schlenk flask and dissolved in dry and degassed DCM (2.0 mL). The clear orange solution was stirred for 2 hours at room temperature and then concentrated to 0.5 mL. Addition of dry and degassed n-pentane (5.0 mL) gave an orange precipitate. The supernatant solution was removed using a filter-tipped cannula, and re-precipitation was repeated another two times. The solids were finally dried in high vacuum to give the desired Rh complex **7b** as a yellow powder (23.3 mg, 16.6 µmol, 74%). The compound exists as two rotamers A and B. ^{31}P{^{1}H} NMR (CDCl$_3$, 161.98 MHz, 300 K): δ = 129.00 (d, ^{1}J(P,Rh) = 179.9 Hz), 129.19 (d, ^{1}J(P,Rh) = 179.8 Hz) ppm. HRMS (ESI): m/z calcd. for C$_{68}$H$_{69}$N$_3$O$_{10}$P$_2$Rh [M-COD-BF$_4$ + CH$_3$CN]$^+$: 1252.35077; found: 1252.34933.

2.13 | Di-tert-butyl 2,2′-((6-(diethylamino)-4,8-dimethoxydibenzo [d,f][1,3,2]dioxaphosphepine-2,10-dicarbonyl)bis(azanediyl)) (2S,2′S)-bis(3-phenylpropanoate) (16)

Selector-modified diol **5a** (100 mg, 135 µmol, 1.00 eq.) was dissolved in dry, degassed, and stabilized THF (2 mL),

and triethylamine (54.6 μL, 391 μmol, 2.90 eq.) was added. The mixture was cooled in an ice bath, and diethylaminophosphoramidous dichloride (22.5 μL, 155 μmol, 1.15 eq.) was added dropwise. The mixture was warmed to room temperature and stirred for 18 hours. For work-up, the mixture was filtered through a filter-tipped cannula, and residual solids were rinsed with more THF (2 × 2 mL). Combined organic washings were evaporated and the crude product was washed with *n*-pentane (3 × 3 mL) to give compound **16** as a white solid (87.0 mg, 103 μmol, 77%). For some atoms, an additional signal splitting was observed. This is caused by the nonequivalence of the two halves in the biphenol-phosphoramidite, which has been previously observed for other chiral phosphoramidites.[39,40] ^1H NMR (THF-d_8, 400.22 MHz, 300 K): δ = 1.05 (t, 3H, $^3J(H,H)$ = 7.0 Hz), 1.40 (s, 9H), 3.05 (dd, 2H, $^3J(P,H)$ = 10.8 Hz, $^3J(H,H)$ = 7.0 Hz), 3.10 (dd, 1H, $^2J(H,H)$ = 13.8 Hz, $^3J(H,H)$ = 8.2 Hz), 3.18 (dd, 1H, $^2J(H,H)$ = 13.8 Hz, $^3J(H,H)$ = 6.5 Hz), 3.87 (s, 3H), 4.78 to 4.84 (m, 1H), 7.14 to 7.18 (m, 1H), 7.23 to 7.29 (m, 4H), 7.48 to 7.49 (m, 1H), 7.58 to 7.59 (m, 1H), 7.81 to 7.84 (m, 1H) ppm. $^{13}C\{^1H\}$ NMR (THF-d_8, 100.65 MHz, 300 K): δ = 14.7, 28.1, 38.6, 38.8, 55.7, 56.2, 81.5, 111.9 (d, $^4J(P,C)$ = 9.6 Hz), 121.0 (d, $^4J(P,C)$ = 12.4 Hz), 127.3, 129.0, 130.2, 131.8, 132.0 (m), 138.6, 144.3 (m), 152.9, 166.6, 171.8 ppm. $^{31}P\{^1H\}$ NMR (THF-d_8, 162.00 MHz, 300 K): δ = 150.9 (quint, $^3J(P,H)$ = 10.8 Hz) ppm. HRMS (ESI): m/z calcd. for $C_{46}H_{57}N_3O_{10}P$ [M + H]$^+$: 842.3776; found: 842.3773. FTIR: ṽ = 697 (s), 740 (s), 843 (s), 1022 (s), 1089 (s), 1151 (s), 1366 (s), 1456 (s), 1533 (m), 1585 (m), 1640 (m), 1733 (m), 2868 (w), 2933 (w), 2974 (m), 3028 (w), 3064 (w), 3088 (w), 3330 (bm) cm^{-1}.

2.14 | [Rh(16)$_2$(COD)]BF$_4$ (17)

Phosphoramidite **16** (150 mg, 178 μmol, 1.00 eq.) and [Rh(COD)$_2$]BF$_4$ (36.2 mg, 89.1 μmol, 0.50 eq.) were dissolved in dry and degassed DCM (5 mL). The orange solution was stirred for 18 hours and subsequently concentrated to 0.5 mL. Addition of *n*-pentane (4 mL) gave the complex as a yellow precipitated. The supernatant solution was removed using a filter-tipped cannula, and the product was re-precipitated another two times. Subsequent drying gave the product as a yellow powder. (141 mg, 71.1 μmol, 80%). Due to high molecular dynamics, very broad signals were observed in ^1H, $^{13}C\{^1H\}$ NMR spectra which made peak assignment impossible. $^{31}P\{^1H\}$ NMR spectrum shows various signals which is in line with the nature of previously investigated Rh complexes of similar nature.[17] $^{31}P\{^1H\}$ NMR (CDCl$_3$, 162.00 MHz, 300 K): δ = 137.6, 138.2, 138.6, 139.3, 140.6, 142.3, 143.7 ppm. HRMS (ESI): m/z calcd. for $C_{100}H_{124}N_6O_{20}P_2Rh$ [M-BF$_4^-$]$^+$:

1894.7429; found: 1894.7464. EA (CHNS): calcd. for $C_{100}H_{124}N_6O_{20}P_2RhBF_4$: C: 60.61, H: 6.31, N: 4.24; found: C: 58.42, H: 6.13, N: 4.23. FTIR: ṽ = 697 (s), 879 (m), 1022 (s), 1153 (s), 1367 (s), 1456 (m), 1527 (m), 1663 (m), 1728 (m), 2872 (w), 2933 (w), 2975 (w), 3314 (bw) cm^{-1}.

2.15 | Additive syntheses

The following compounds are known in literature and were prepared accordingly: (*S/R*)-2-acetamido-*N*-methyl-3-phenylpropanamide (**10**),[41] (*S*)-2-acetamido-*N*-methylpropanamide (**12**)[41], and (*S*)-*N*-(1-(*tert*-butylamino)-1-oxo-3-phenylpropan-2-yl)benzamide (**13**)[30]. In all cases where gaseous amines were supposed to be employed, these were substituted by their respective alcoholic solutions.

2.16 | (*S*)-2-acetamido-*N*-(3,5-dichlorophenyl)propanamide (11)

(*S*)-*N*-Acetyl alanine (200 mg, 1.53 mmol, 1.00 eq.) was suspended in dry DCM (5 mL). EDCI.HCl (322 mg, 1.68 mmol, 1.10 eq.) was added, and the mixture was stirred for 15 minutes to give a clear solution. Subsequently, 3,5-dichloroaniline (260 mg, 1.60 mmol, 1.05 eq.) was added as a solid to give a dark purple solution from which solids precipitated shortly after. After 16 hours, the solids were collected by filtration. The mother liquor was evaporated, and the residue slurried in warm acetonitrile from which another batch of solids was obtained. The combined crude product was finally dissolved in ethyl acetate (10 mL) at 65°C and crystallized in the freezer. This was repeated twice to give the enantiomerically pure product as a white, crystalline solid (150 mg, 1.53 mmol, 36%). The enantiopurity of the compound was verified by chiral HPLC (Chiralpak IA, hexane:isopropanol 80:20, t_R = 5.10 min) and was found to be >99% ee. ^1H-NMR (CD$_3$OD, 600.24 MHz, 300 K): δ = 1.26 (d, 3H, $^3J(H,H)$ = 7.0 Hz), 1.85 (s, 3H), 4.31 (dt, 1H, $^3J(H,H)$ = 7.0 Hz, $^3J(H,NH)$ = 6.9 Hz), 7.27 (t, 1H, $^3J(H,H)$ = 1.8 Hz), 7.67 (d, 2H, $^3J(H,H)$ = 1.8 Hz), 8.24 (d, 1H, $^3J(NH,H)$ = 6.9 Hz), 10.33 (s, 1H) ppm. $^{13}C\{^1H\}$-NMR (CD$_3$OD, 150.93 MHz, 300 K): δ = 17.7, 22.4, 49.3, 117.4, 122.6, 134.1, 141.3, 169.4, 172.4 ppm. HRMS (ESI): m/z calcd. for $C_{11}H_{12}Cl_2N_2NaO_2$ [M + Na]$^+$: 297.0168; found: 297.0170. FTIR: ṽ = 668 (s), 1153 (s), 1409 (s), 1436 (s), 1526 (s), 1586 (s), 1642 (s), 2978 (w), 3086 (w), 3117 (w), 3181 (w), 3257 (w), 3343, (m) cm^{-1}. [α]$_D^{20}$-34.9 (c 0.5%, MeOH).

2.17 | (R)-N-(1-(tert-butylamino)-1-oxo-3-phenylpropan-2-yl)benzamide (13)

This compound was prepared according to the same procedure as its enantiomer, which has already been reported elsewhere.[30] Analytical NMR and HR-MS data was identical. Analytics for BOC-protected amide: $[\alpha]_D^{20}$ −9.0 (c 1% in CHCl₃). Analytics for amide hydrochloride: $[\alpha]_D^{20}$ −67.3 (c 1% in CHCl₃). Analytics for diamide: $[\alpha]_D^{20}$ −7.2 (c 1% in CHCl₃).

2.18 | (S)-2-acetamido-N-(3-nitrophenyl)propanamide (15)

(S)-N-acetyl alanine (400 mg, 3.05 mmol, 1.00 eq.) was placed in a dried Schlenk flask and suspended in dry DCM (2 mL). The mixture was cooled in an ice bath, and EDCI.HCl (643 mg, 3.36 mmol, 1.10 eq.) was added as a solid. After 15 minutes, all solids had dissolved, and 3-nitroaniline (421 mg, 3.05 mmol, 1.00 eq.) was added. After stirring was continued for another 18 hours at room temperature, the solution was diluted more DCM (50 mL). The organic layer was washed with HCl solution (2 M, 3 × 50 mL), saturated bicarbonate solution (2 × 50 mL), and brine (1 × 50 mL), dried over sodium sulfate, and evaporated. Resulting solids were recrystallized four times from hot ethyl acetate at 60°C to give the enantiopure product as a white powder (300 mg, 1.19 mmol, 39 %). Enantiopurity of the compound was confirmed by chiral HPLC (Chiralpak IE, hexane:isopropanol 80:20, 1 mL/min, 20°C, t_R = 8.3 min). ¹H NMR (DMSO-d6, 400.33 MHz, 300 K): δ = 1.30 (d, 3H, ³J(H,H) = 7.1 Hz), 1.87 (s, 3H), 4.37 (dq, 1H, ³J(H,H) = 7.1 Hz, ³J(H,H) = 7.0 Hz), 7.60 (t, 1H, ³J(H,H) = 8.2 Hz), 7.89 to 7.94 (m, 2H), 8.23 (d, 1H, ³J(H,H) = 6.9 Hz), 8.64 (t, 1H, ⁴J(H,H) = 2.2 Hz), 10.46 (s, 1H) ppm. ¹³C{¹H} NMR (DMSO-d6, 100.66 MHz, 300 K): δ = 17.7, 22.4, 49.3, 113.3, 117.8, 125.2, 130.2, 140.1, 148.0, 169.4, 172.3 ppm. HRMS (ESI): m/z calcd. for $C_{22}H_{26}N_6NaO_8$ [M + Na]⁺ 525.1704; found: 525.1713. FTIR: ṽ = 729 (s), 740 (s), 820 (s), 1209 (s), 1294 (s), 1345 (s), 1526 (s), 1599 (s), 1647 (s), 1686 (s), 2950 (w), 3001 (w), 3103 (bm), 3136 (w), 3246 (m) cm⁻¹. $[\alpha]_{880nm}^{20}$ −1.3 (c 1%, MeOH).

2.19 | (Z)-4-benzylidene-2-phenyloxazol-5(4H)-one (18)

Hippuric acid (25 g, 139 mmol, 1 eq.), benzaldehyde (21.9 g, 2.07 mmol, 1.48 eq.), sodium acetate (8.47 g, 103 mmol, 0.74 eq.), and acetic anhydride (33.0 mL, 349 mmol, 2.50 eq.) were mixed and heated to 140°C for 2 hours and yellow solid formed. The product was filtered off, washed with water (3 × 75 mL), and recrystallized from methanol to yield the product as a yellow solid (21.5 g, 86.3 mmol, 62 %). ¹H NMR (CDCl₃, 400.22 MHz, 300 K): δ = 7.25 (s, 1H), 7.46 to 7.55 (m, 5H), 7.60 to 7.64 (m, 1H), 8.18 to 8.22 (m, 4H) ppm. ¹³C{¹H} NMR (CDCl₃, 100.65 MHz, 300 K): δ = 125.7, 128.5, 129.0, 129.1, 131.4, 131.9, 132.6, 133.4, 133.5, 133.6, 163.6, 167.8 ppm. HRMS (EI): m/z calcd. for $C_{16}H_{12}NO_2$ [M + H]⁺: 250.08626; found: 250.08642. FTIR: ṽ = 684 (s), 766 (s), 983 (s), 1294 (s), 1448 (s), 1651 (s), 1791 (s), 3028 (w), 3242 (w) cm⁻¹.

2.20 | (Z)-N-(3-(tert-butylamino)-3-oxo-1-phenylprop-1-en-2-yl)-benzamide (19)

Azlactone 18 (800 mg, 3.21 mmol, 1.00 eq.) was dissolved in chloroform (20 mL). The clear solution was cooled in an ice bath and treated with tert-butylamine (3.37 mL, 32.1 mmol, 10.00 eq.). The clear solution was subsequently stirred at 40°C for 72 hours. For work-up, all volatiles were removed in vacuo, and residual off-white solids were recrystallized from acetone:hexane to give the product as a white solid (702 mg, 2.18 mmol, 68%). ¹H NMR (CDCl₃, 400.22 MHz, 300 K): δ = 1.30 (s, 9H), 6.17 (s, 1H), 6.73 (s, 1H), 7.13 to 7.22 (m, 3H), 7.28 to 7.34 (m, 4H), 7.40 to 7.44 (m, 1H), 7.74 (d, 2H, ³J(H,H) = 7.3 Hz), 8.08 (s, 1H) ppm. ¹³C{¹H} NMR (CDCl₃, 100.65 MHz, 300 K): δ = 28.7, 51.8, 125.3, 127.8, 128.7, 128.8, 128.9, 129.1, 131.1, 132.3, 133.2, 134.1, 165.5, 166.3 ppm. HRMS (EI): m/z calcd. for $C_{20}H_{22}N_2O_2$ [M]⁺: 322.1681; found: 322.1678. FTIR: ṽ = 688 (s), 1223 (s), 1281 (s), 1475 (s), 1627 (s), 1642 (s), 2871 (w), 2826 (w), 2967 (m), 3029 (w), 3059 (m), 3238 (bm) cm⁻¹.

2.21 | Hydrogenation experiments

For hydrogenation experiments with bisphosphinite catalysts 7a and 7b, methyl 2-acetamidoacrylate 8 (6.10 mg, 42.6 µmol, 20 eq. with respect to catalyst) was added to the equilibrated mixtures from the seeding experiments (see SI section 2.3). For hydrogenation experiments with phosphoramidite catalyst 17 and substrate 8, a J. Young NMR tube was charged with a 3.2 Mm stock solution of the catalyst, as well as appropriate amounts of substrate (20 eq.) and additive (10 eq for (S)- or (R)-13, 20 eq. for rac-13). The catalyst was added from a stock solution. For those experiments with catalyst 17 and olefin 19, a catalyst stock solution of the desired concentration was prepared and added to a J. Young NMR tube together with the substrate, whose amount was adjusted to account for catalyst loading of the respective reaction. The prepared solution was transferred into a nitrogen filled stainless steel reactor loaded with a standard NMR

tube and a small stirring bar. The reactor was pressurized with hydrogen gas (50 bar in case of bisphosphinite complexes, 5 bar in case of phosphoramidite complexes, unless noted otherwise) to initiate the catalysis. The autoclave was reopened after one day (two days in case of low catalyst concentrations). The solution was passed through a short pipet filled with silica (ca. 3 cm) using ethyl acetate as eluent. Evaporation gave the hydrogenation product as a yellow oil. Enantiomeric ratio and conversion were determined by chiral GC (compound **9**: (6-TBDMS-2,3-Ac)-β-CD, 25 m, i.d. 250 μm, film thickness 250 nm, prepared and coated in the Trapp group, 100-kPa helium, 130°C, FID detection, $k_{Subst} = 4.59$, $k_R = 6.63$, $k_S = 8.76$, α (k_S/k_R) = 1.32) or chiral HPLC (compound **19**: Chiralpak IE, hexane:isopropanol: 80:20, 1 mL/min, 20°C, 254 nm, $t_S = 5.3$ min and $t_R = 5.9$ min, $t_{Subst} = 15.1$ min). Assignment of absolute configuration was accomplished by comparing measurements to those of previously prepared enantiopure samples. The conversion of all hydrogenation reactions was greater 99.5%, and no byproducts were observed.

3 | RESULTS AND DISCUSSION

3.1 | Interaction studies

Initial interaction studies were to be conducted on stereodynamic bisphosphinite ligands, as their rhodium complexes have a rotational barrier above 80 kJ mol^{-1} which allows for a distinct differentiation of the two axial isomers by NMR spectroscopy, while equilibration of the ligand still occurs at ambient temperature.[33] Furthermore, the direct relationship between rotamer distribution and enantioselectivity in asymmetric hydrogenation reactions is known.[42] Ligand synthesis was achieved by initial oxidative coupling of methyl vanillate **1**, protection of the resulting 2,2′-biphenol with allyl bromide and saponification of the methyl ester groups of **2** to yield dicarboxylic acid **3** (see Figure 2).

After introduction of the selector units by reaction of the corresponding diacid chloride with the respective amine hydrochloride (**4a**) or by Steglich esterification (**4b**), palladium-mediated deprotection of the hydroxyl groups with formic acid gave biphenols **5a,b**. Finally, reaction with PPh$_2$Cl afforded the bisphosphinite ligands **6a,b**, which were treated with [Rh (COD)$_2$]BF$_4$ to give the desired catalysts **7a,b**.

A comparison of both ligand types revealed significant differences.[34] Rh complex **7b**, which was formed as a mixture of two axial rotamers of equal amounts, could not be influenced by addition of chiral additives (see SI for spectral data; cf. Figure S4), and subsequent
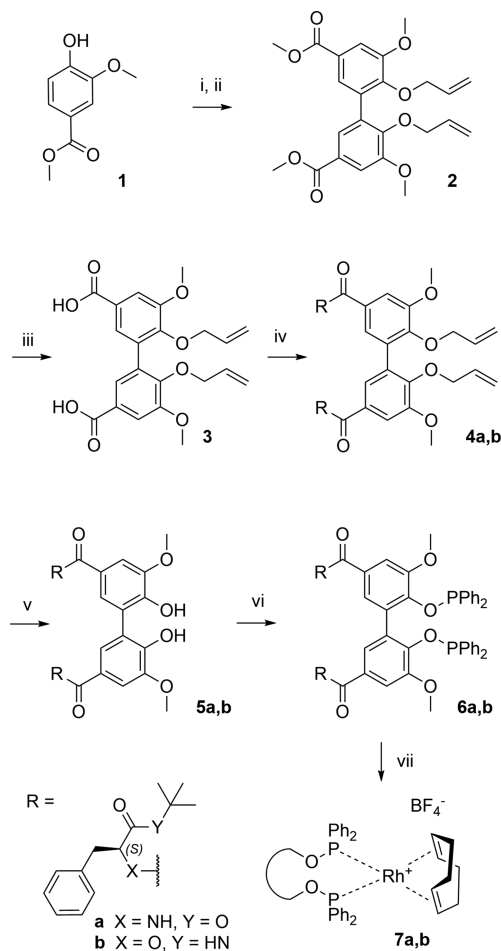

FIGURE 2 Synthesis of selector-modified rhodium catalysts **7a,b**
i) PhI (OAc)$_2$, 51%, ii) allyl bromide, K$_2$CO$_3$, 97%, iii) KOH, 99%, iv) **a**: SOCl$_2$, then NH$_3$Cl-(S)-Phe-O^{t}Bu, DIPEA, 91%; **b**: HO-(S)Phe-NH^{t}Bu (**S1**), DMAP, EDCI·HCl, 50%, v) Pd (OAc)$_2$, PPh$_2$ (C$_6$H$_4$NMe$_2$), HCOOH, **a**: 71%; **b**: 93% vi) **a**: PPh$_2$Cl, DABCO, 20%; **b**: PPh$_2$Cl, triethylamine, 69%, vii) [Rh (COD)$_2$]BF$_4$, quant

asymmetric hydrogenation experiments of methyl 2-acetamidoacrylate **8** generated exclusively racemates. For compound **7a**, however, a weighted equilibrium of both rotamers was found comprising a major R_{ax} and a minor S_{ax} rotamer (for assignment of rotamers, see SI; cf. Figure S3). When N-acetyl (S)-phenylalanine methyl amide (S)-**10** was added to the complex in excess, a significant rotameric enrichment of R_{ax}-**7a** was observed by ^{31}P NMR spectroscopy (see Figure 3). The enrichment process took several hours and was accompanied by an immediate low-field shift and distinct sharpening of the NMR signals for the increasing rotamer. Interestingly, signals representing the minor species S_{ax}-**7a** showed only a negligible change. In the following, similar ligand enrichment was also found during the addition of other amino acid derivatives of the same configuration (see SI for spectral data).
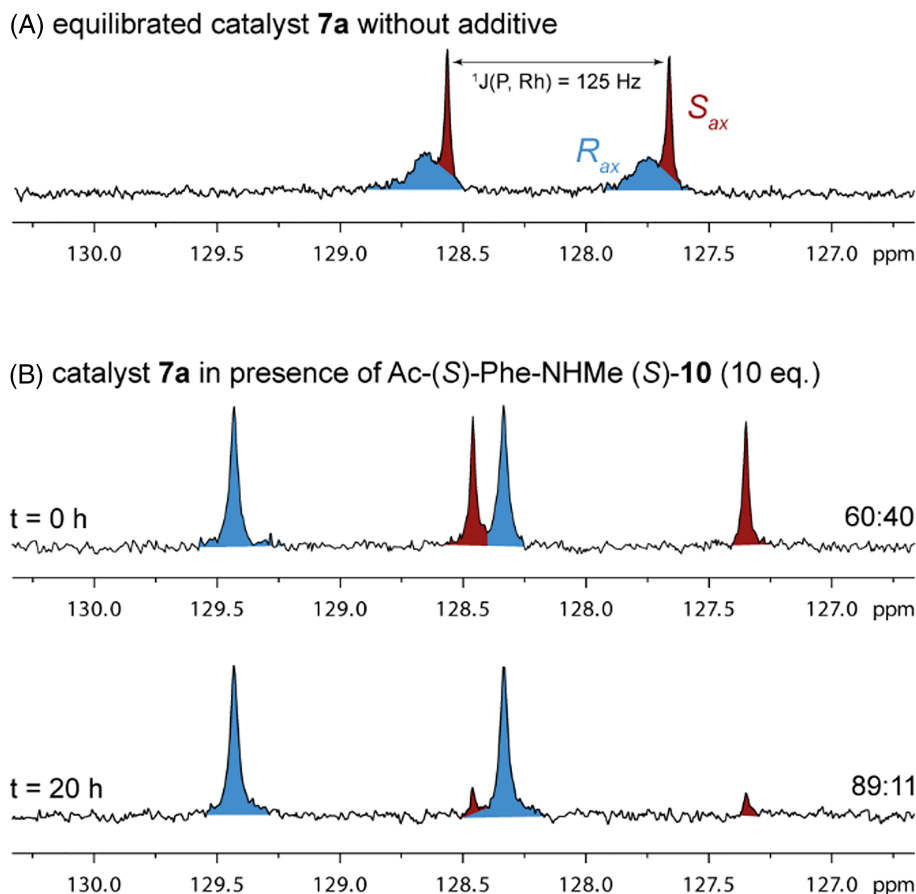
FIGURE 3 ^{31}P NMR spectra showing influence of *N*-acetyl phenylalanine methyl amide (*S*)-**10** on rhodium complex **7a** (4.3 mM in CDCl$_3$). Noncovalent interactions between the additive (10 eq.) and the ligand's interaction sites induce rotameric enrichment of R_{ax}-**7a** during re-equilibration over several hours at 20°C

In some cases, signal overlap and line broadening, caused by noncovalent interactions, did not allow for an unambiguous determination of the final rotameric distribution of **7a**. Therefore, hydrogenation experiments were carried out, and stereoenriched complex mixtures were used as catalysts in order to comparatively assess the structural adaptation of the ligand resulting from the noncovalent interactions (see Figure 4). The untreated catalyst converted methyl 2-acetamidoacrylate **8** to alanine methyl ester **9** with an enantiomeric excess of 27% *ee R*. All (*S*)-amino acid-derived additives were found to align the catalyst to significantly increase its selectivity. Additionally, enantiomeric discrimination during ligand-additive interaction was observed. In the presence of (*S*)-**10**, a strong NMR signal shift as well as significant rotameric enrichment was observed for the major rotamer of complex **7a** and selectivity for hydrogenation of **8** increased to 56% *ee R* ($\Delta ee = +29\%$). (*R*)-**10**, however, induced no visible change to the catalyst, and the difference in selectivity generated during subsequent catalysis was negligible (29% *ee R*, $\Delta ee = +2\%$). Strongest stereoinduction was found using alanine derivatives with

electron-deficient aromatics at the *N*-terminus, Ac-(*S*)-Ala-NH-(3,5-dichlorophenyl) **11** and Ac-(*S*)-Ala-NH-(3-nitrobenzene) **15**, which, after catalyst alignment, allowed reduction of **8** with 84% *ee R* ($\Delta ee = +57\%$) and 81% *ee R* ($\Delta ee = +54\%$), respectively, and selector-like diamide (*S*)-**13**, which increased selectivity during hydrogenation to 82% *ee R* ($\Delta ee = +55\%$).

3.2 | Autoinductive hydrogenation

Following the successful demonstration of chirality transfer, these results were utilized in the second phase to realize an asymmetric hydrogenation reaction that is governed by enantioselective self-inhibition.[34] Since bisphosphinite complex **7a,** discussed above, took numerous hours to equilibrate in the presence of chiral additives, a rhodium complex bearing highly dynamic phosphoramidite ligand with the same ligand core as ligand **6a** was synthesized (see Figure 5A). This compound was expected to instantly adapt to a changing chiral environment, due to its low barrier of rotation.[17]
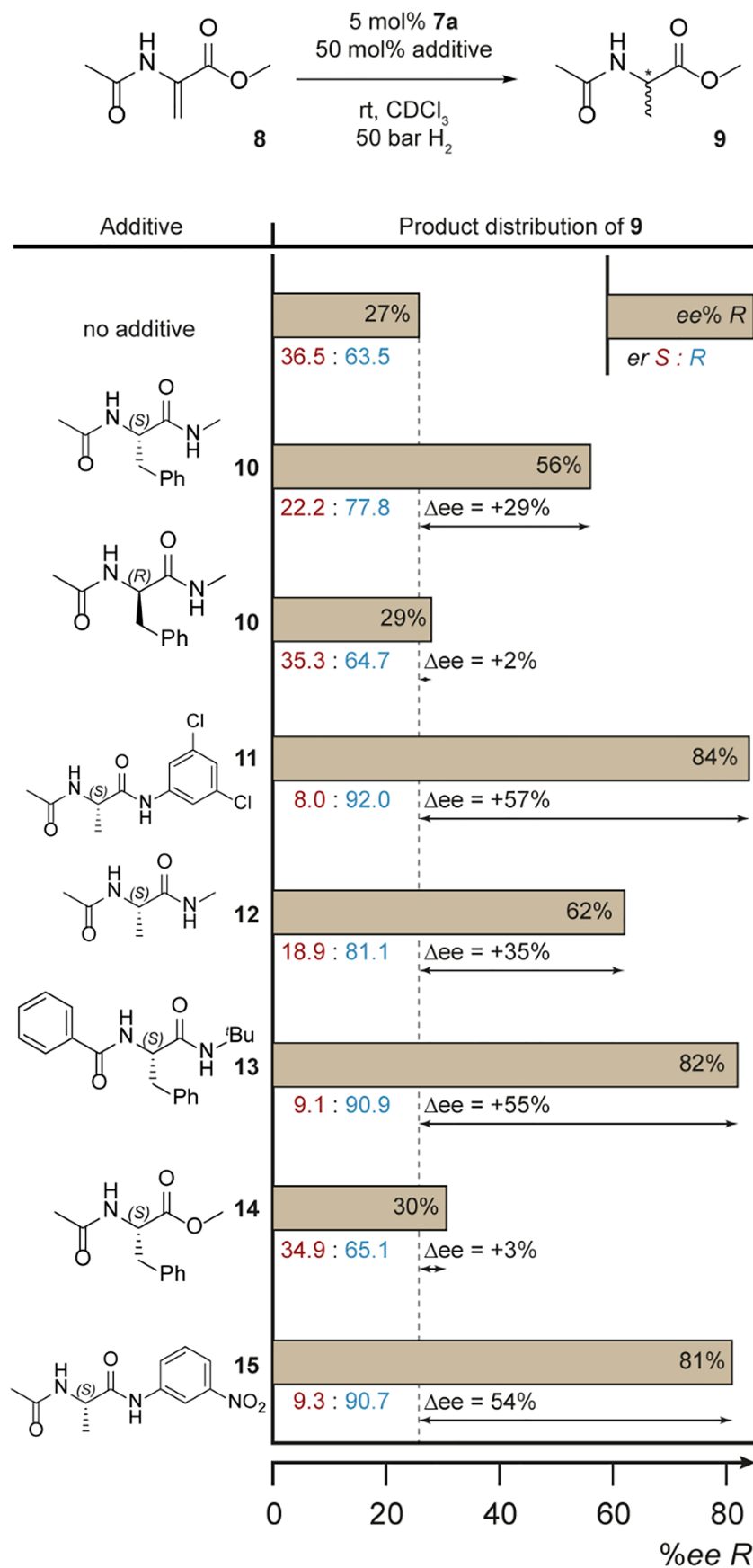
FIGURE 4 Hydrogenation experiments with catalyst **7a**, which was pre-aligned using various chiral amino acid derivatives. Adaptation of the ligand's rotamer ratio during interactions with certain additives is illustrated by a concurrent change in the catalyst's selectivity. All reactions showed full conversion. A detailed experimental procedure can be found in the experimental section.
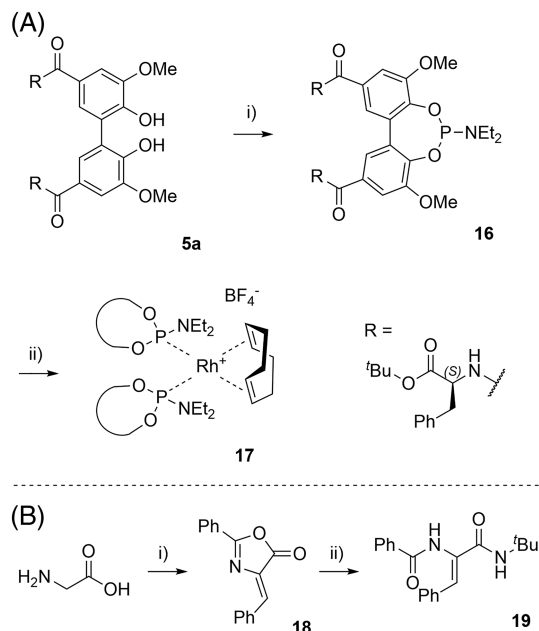
FIGURE 5 (A) Synthesis of stereodynamic complex **17**: i) Cl$_2$PNEt$_2$, NEt$_3$, 77%, ii) [Rh (COD)$_2$]BF$_4$, *quant.* (B) Synthesis of prochiral olefin **19** i) PhCOCl, PhCHO, NaOAc, 62%, ii) ^{t}BuNH$_2$, 68%

FIGURE 6 Stereodynamic, phosphoramidite-bearing catalyst **17** shows a change in selectivity in presence of the *S* enantiomer of additive **13**. All reactions showed full conversion. A detailed experimental procedure can be found in the SI

Regarding the appropriate substrate for an autoinductive reaction, good solubility as well as high stereoinductive capacities for the corresponding hydrogenated product was considered important. Electron-deficient alanine derivatives (*S*)-**11** and (*S*)-**15** were already only sparingly soluble, and olefin analogs usually exhibit reduced solubility. Consequently, phenylalanine-derived diamide (*S*)-**13** was chosen, whose olefin counterpart **19** could be conveniently synthesized from glycine, benzoic acid chloride, and benzaldehyde with subsequent aminolysis in *tert*-butylamine (see Figure 5B).

As with previously investigated phosphoramidite complexes bearing amino acid-derived selector moieties, compound **17** was found to produce a complex ^{31}P NMR spectrum indicating an equilibrium of various species (see SI in Storch and Trapp 17 for further information). In the presence of the enantiomers of diamide **13**, again, stereoselective interaction with the catalyst was observed by NMR spectroscopy (see SI for spectral data; cf. Figures S1, S2 and S5). When employing these catalyst mixtures for the asymmetric hydrogenation of prochiral olefin **8**, a change in selectivity was found when the *S* enantiomer or the racemate of **13** was present. Sole addition of the *R* enantiomer gave almost no change for the enantiomeric ratio of alanine derivative **9** (see Figure 6). These results demonstrate that findings of stereoselective interactions and resulting stereoinduction concerning bisphosphinite **6a** can also be applied to the more dynamic phosphoramidite analogue **16**.
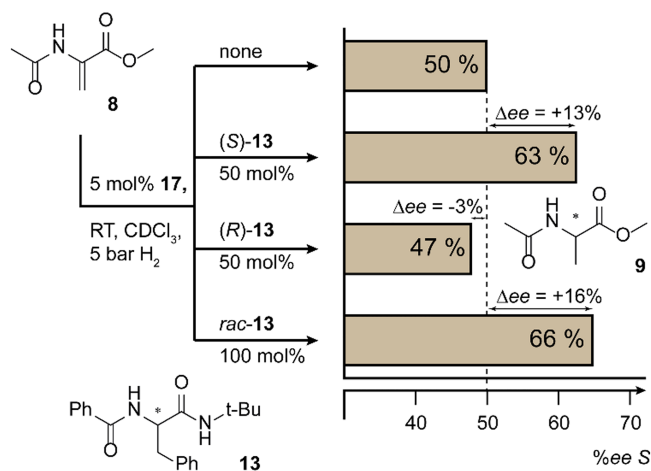
With these results at hand, a first set of hydrogenation experiments with substrate **19** using different catalyst loadings at a constant catalyst concentration were conducted. As this associates with different turnover numbers (TONs)[43], a decreased catalyst loading results in an
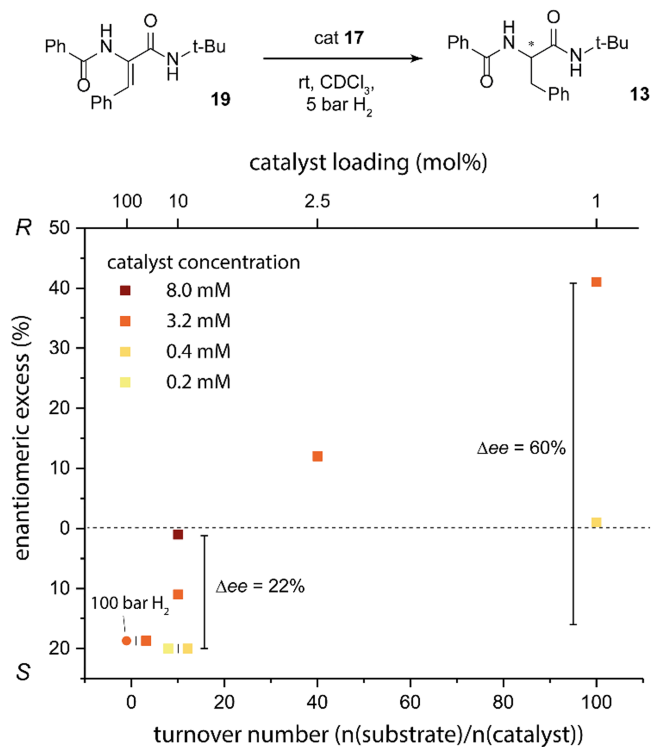

FIGURE 7 Results for the reduction of olefin **19** to phenylalanine derivative **13** using stereodynamic catalyst **17**. Selectivities were found to depend on the turnover number and the concentration of the catalyst. The change of product *ee* is indicated. All reactions showed full conversion. A detailed experimental procedure can be found in the experimental section.

increase in catalytic cycles, which is equivalent to higher levels of interaction between the catalyst and an increasing amount of formed product molecules. This modifies dynamically the catalyst's structure as well as its selectivity, which changes in course of the turn over steps, and hence changes the enantiomeric excess of the final product over time. The results are summarized in Figure 7. With 100 mol% catalyst, which corresponds to a TON of 1, at 5 bar H_2, selectivity for **13** was found to be 19% *ee* in favor of the *S* enantiomer. The same outcome was observed when the reaction was repeated with 100 bar H_2 gas. This affirms that the selectivity of the reduction is determined by the distribution of stereo-dictating species of compound **17** and not the result of diastereoselective catalyst activation, ie, kinetically favored hydrogenation of cyclooctadiene for a specific catalyst species. Decreasing the catalyst loading led to a significant change in selectivity. Running the reaction with 10 mol% catalyst (TON = 10) gave product **13** with a slightly lower excess for the *S* enantiomer of 10%. When 2.5 mol% and 1 mol% catalyst (TON = 40 and TON = 100, respectively) were used, a reversal of selectivity was observed, and diamide **13** was obtained in 12% *ee R* and 41% *ee R*, respectively. This represents an overall shift in selectivity of $\Delta ee = 60\%$ toward the *R* enantiomer. When a similar set of experiments was repeated with substrate **8**, however, a change of the TON always yielded the same enantiomeric ratio of product **9**, which, similar to previously investigated amido ester **14**, was not believed to have any influence on the selectivity of the reaction. This demonstrates that the enantioselectivity of catalyst **17** is not inherently dependent on its TON. However, (*S*)-**13**, as previously established, is capable of inducing structural change to the catalyst to alter its selectivity. Increased production of the *R* enantiomer with higher TONs thus demonstrates that the original major enantiomer (*S*)-**13** triggers the enrichment of its mirror and suppresses its own formation over the course of the reaction.

In a following set of experiments, hydrogenations were repeated with varying catalyst concentrations and a constant catalyst loading of 10 mol%. Selectivity changed from 23% *ee S* to 1% *ee S* ($\Delta ee = 22\%$) when the concentration was increased from 0.2 to 8 mM with respect to the catalyst. This was attributed to intermolecular interactions between different catalyst molecules. The interaction site of one molecule acts as chiral additive to align a neighboring biphenyl unit. This behavior was also observed for bisphosphinite ligand **6a** (see SI section 2.1 for details about ligand-ligand interaction). An increased presence of selector units with *S* configuration evoked the same trend of change for the reaction's selectivity compared with (*S*)-**13**, which appears reasonable given their structural similarity.

4 | CONCLUSION

In summary, a novel (*S*)-phenylalanine-based amido ester selector unit for noncovalent interaction has been successfully used with a variety of differently substituted amino acid-derived additives to induce chirality in a stereodynamic bisphosphinite catalyst (**7a**) to enhance selectivity in the asymmetric hydrogenation of methyl 2-acetamidoacrylate **8**. Selectivity could be increased from 27% *ee R*, when no additive was present, to 84% *ee R* ($\Delta ee = 57\%$) when Ac-(*S*)-Ala-NH-(3,5-dichlorophenyl) **11** was used as stereoinducing additive.

On the basis of these findings, highly stereodynamic catalyst **17** and olefin **19**, which was derived of strongly interacting diamide PhCO-(*S*)-Phe-NHtBu (*S*)-**13**, were synthesized. During asymmetric hydrogenation of this olefin, it was demonstrated that the initially preferred product enantiomer (*S*)-**13** interacted with the catalyst **17** to suppress its own formation. Ongoing enantioselective self-inhibition leads to increased production of the R enantiomer and selectivity changed from 19% *ee S*, using 100 mol% catalyst, to 41% *ee R*, when 1 mol% catalyst was used ($\Delta ee = 60\%$). A second parameter found to influence the catalyst's behavior was its concentration, which was linked to weak intermolecular interactions between selector units of different catalyst molecules. (*S*)-**13**-like interaction sites align neighboring biphenyl units thus enhancing enantioselectivity for the formation of (*R*)-**13** with increased concentration of catalyst **17**. Ultimately, these resultes illustrate how stereoselective self-inhibition, a process that controls a large number of biochemical systems in nature, can be recreated on a molecular level.

ORCID

Oliver Trapp https://orcid.org/0000-0002-3594-5181

REFERENCES

1. Todd MH. Asymmetric autocatalysis: product recruitment for the increase in the chiral environment (PRICE). *Chem Soc Rev.* 2002;31(4):211-222.

2. Satyanarayana T, Abraham S, Kagan HB. Nonlinear effects in asymmetric catalysis. *Angew Chem Int Ed.* 2009;48(3):456-494.

3. Puchot C, Samuel O, Dunach E, Zhao S, Agami C, Kagan HB. Nonlinear effects in asymmetric synthesis. Examples in

asymmetric oxidations and aldolization reactions. *J Am Chem Soc.* 1986;108(9):2353-2357.

4. Guillaneux D, Zhao S-H, Samuel O, Rainford D, Kagan HB. Nonlinear effects in asymmetric catalysis. *J Am Chem Soc.* 1994;116(21):9430-9439.

5. Kitamura M, Okada S, Suga S, Noyori R. Enantioselective addition of dialkylzincs to aldehydes promoted by chiral amino alcohols. Mechanism and nonlinear effect. *J Am Chem Soc.* 1989;111(11):4028-4036.

6. Aikawa K, Mikami K. Asymmetric catalysis based on tropos ligands. *Chem Commun.* 2012;48(90):11050-11069.

7. Mikami K, Terada M, Korenaga T, Matsumoto Y, Ueki M, Angelaud R. Asymmetric activation. *Angew Chem Int Ed.* 2000;39(20):3532-3556.

8. Mikami K, Yamanaka M. Symmetry breaking in asymmetric catalysis: racemic catalysis to autocatalysis. *Chem Rev.* 2003;103(8):3369-3400.

9. Frank FC. On spontaneous asymmetric synthesis. *Biochim Biophys Acta.* 1953;11:459-463.

10. Wynberg H, Feringa B. Enantiomeric recognition and interactions. *Tetrahedron.* 1976;32(22):2831-2834.

11. Alberts AH, Wynberg H. The role of the product in asymmetric carbon-carbon bond formation: stoichiometric and catalytic enantioselective autoinduction. *J Am Chem Soc.* 1989;111(18):7265-7266.

12. Danda H, Nishikawa H, Otaka K. Enantioselective autoinduction in the asymmetric hydrocyanation of 3-phenoxybenzaldehyde catalyzed by cyclo[(R)-phenylalanyl-(R)-histidyl]. *J Org Chem.* 1991;56(24):6740-6741.

13. Shvo Y, Gal M, Becker Y, Elgavi A. Asymmetric hydrocyanation of aldehydes with cyclo-dipeptides: a new mechanistic approach. *Tetrahedron: Asymmetry*. 1996;7(3):911-924.

14. Szlosek M, Figadère B. Highly enantioselective aldol reaction with 2-trimethylsilyloxyfuran: the first catalytic asymmetric autoinductive aldol reaction. *Angew Chem Int Ed.* 2000;39(10):1799-1801.

15. Sato I, Urabe H, Ishiguro S, Shibata T, Soai K. Amplification of chirality from extremely low to greater than 99.5% ee by asymmetric autocatalysis. *Angew Chem Int Ed.* 2003;42(3):315-317.

16. Soai K, Shibata T, Morioka H, Choji K. Asymmetric autocatalysis and amplification of enantiomeric excess of a chiral molecule. *Nature.* 1995;378(6559):767-768.

17. Storch G, Trapp O. By-design enantioselective self-amplification based on non-covalent product-catalyst interactions. *Nat Chem.* 2017;9(2):179-187.

18. Maier F, Trapp O. Effects of the stationary phase and the solvent on the stereodynamics of biphep ligands quantified by dynamic three-column HPLC. *Angew Chem Int Ed.* 2012;51(12):2985-2988.

19. Maier F, Trapp O. The stereodynamics of 5,5′-disubstituted BIPHEPs. *Chirality.* 2013;25(2):126-132.

20. Storch G, Maier F, Wessig P, Trapp O. Rotational barriers of substituted BIPHEP ligands: a comparative experimental and theoretical study. *Eur J Org Chem.* 2016;2016(30):5123-5126.

21. Storch G, Trapp O. Temperature-controlled bidirectional enantioselectivity in a dynamic catalyst for asymmetric hydrogenation. *Angew Chem Int Ed.* 2015;54(12):3580-3586.

22. Siebert M, Storch G, Rominger F, Trapp O. Temperature-controlled bidirectional enantioselectivity in asymmetric hydrogenation reactions utilizing stereodynamic iridium complexes. *Synthesis.* 2017;49(15):3485-3494.

23. Storch G, Deberle L, Menke J-M, Rominger F, Trapp O. A stereodynamic phosphoramidite ligand derived from 3,3′-functionalized ortho-biphenol and its rhodium(I) complex. *Chirality.* 2016;28(11):744-748.

24. Storch G, Pallmann S, Rominger F, Trapp O. Stereodynamic tetrahydrobiisoindole "NU-BIPHEP(O)"s: functionalization, rotational barriers and non-covalent interactions. *Beilstein J Org Chem.* 2016;12:1453-1458.

25. Storch G, Siebert M, Rominger F, Trapp O. 5,5′-Diamino-BIPHEP ligands bearing small selector units for non-covalent binding of chiral analytes in solution. *Chem Commun.* 2015;51(86):15665-15668.

26. Pirkle WH, Murray PG, Rausch DJ, McKenna ST. Intermolecular 1H−1H two-dimensional nuclear Overhauser enhancements in the characterization of a rationally designed chiral recognition system. *J Org Chem.* 1996;61(14):4769-4774.

27. Pirkle WH, Murray PG. An instance of temperature-dependent elution order of enantiomers from a chiral brush-type HPLC column. *J High Resolut Chromatogr.* 1993;16(5):285-288.

28. Pirkle WH, Murray PG, Wilson SR. X-ray crystallographic evidence in support of a proposed chiral recognition mechanism. *J Org Chem.* 1996;61(14):4775-4777.

29. Scholtes JF, Trapp O. Inducing enantioselectivity in a dynamic catalyst by supramolecular interlocking. *Angew Chem Int Ed.* 2019;58(19):6306-6310.

30. Scholtes JF, Trapp O. Supramolecular interlocked biphenyl ligands for enantioselective Ti-catalyzed alkylation of aromatic aldehydes. *Organometallics.* 2019. https://doi.org/10.1021/acs.organomet.9b00262

31. Storch G, Haas M, Trapp O. Attracting enantiomers: chiral analytes that are simultaneously shift reagents allow rapid screening of enantiomeric ratios by NMR spectroscopy. *Chem. Eur. J.* 2017;23(23):5414-5418.

32. Maier F, Trapp O. Selector-induced dynamic deracemization of a selectand-modified tropos BIPHEPO-ligand: application in the organocatalyzed asymmetric double-aldol-reaction. *Angew Chem Int Ed.* 2014;53(33):8756-8760.

33. Storch G, Trapp O. Supramolecular chirality transfer in a stereodynamic catalysts. *Chirality.* 2018;30(10):1150-1160.

34. Scholtes JF. Chiral induction in stereodynamic catalysts by non-covalent interactions. PhD Thesis. Ludwig-Maximilians-Universität München; 2019.

35. Fulmer GR, Miller AJM, Sherden NH, et al. NMR chemical shifts of trace impurities: common laboratory solvents, organics, and gases in deuterated solvents relevant to the organometallic chemist. *Organometallics.* 2010;29(9):2176-2179.

36. Kaneko K, Miwa Y, Nakamura N. Phase transition behavior and electro-rheological effect of liquid crystalline cyclic-siloxanes with fluorine atoms. *J Appl Polym Sci.* 2007;105(5):2474-2481.

37. Wells G, Seaton A, Stevens MF. Structural studies on bioactive compounds. 32. Oxidation of tyrphostin protein tyrosine kinase inhibitors with hypervalent iodine reagents. *J Med Chem.* 2000;43(8):1550-1562.

38. Hey H, Arpe HJ. Removal of allyl groups by formic-acid catalyzed by (triphenylphosphane)palladium. *Angew Chem Int Ed.* 1973;12(11):928-929.

39. Monti C, Gennari C, Piarulli U, de Vries JG, de Vries AH, Lefort L. Rh-catalyzed asymmetric hydrogenation of prochiral olefins with a dynamic library of chiral TROPOS phosphorus ligands. *Chem. Eur. J.* 2005;11(22):6701-6717.

40. de Vries AHM, Meetsma A, Feringa BL. Enantioselective conjugate addition of dialkylzinc reagents to cyclic and acyclic enones catalyzed by chiral copper complexes of new phosphorus amidites. *Angew Chem Int Ed.* 1996;35(20):2374-2376.

41. Applewhite TH, Niemann C. The interaction of α-chymotrypsin with a series of α-N-acetyl-α-amino acid methylamides1. *J Am Chem Soc.* 1959;81(9):2208-2213.

42. Zhou Y-G, Zhang X. Synthesis of novel BINOL-derived chiral bisphosphorus ligands and their application in catalytic asymmetric hydrogenation. *Chem Commun.* 2002;(10): 1124-1125.

43. TON is referred to here as the quotient n (substrate)/n (catalyst). Partial catalyst activation was experimentally addressed, but is formally not considered.

SUPPORTING INFORMATION

Additional supporting information may be found online in the Supporting Information section at the end of the article.

How to cite this article: Scholtes JF, Trapp O. Design and synthesis of a stereodynamic catalyst with reversal of selectivity by enantioselective self-inhibition. *Chirality.* 2019;31:1028–1042. https://doi.org/10.1002/chir.23132